Title

Two-oscillator model of ventilatory rhythmogenesis in the frog

Journal

Neurocomputing, 65(SPEC. ISS.)

ISSN

0925-2312

Authors

Bose, Amitabha
Lewis, Timothy J
Wilson, Richard JA

Publication Date

2005-06-01

DOI

10.1016/j.neucom.2004.10.071

Peer reviewed

Available online at www.sciencedirect.com
SCIENCE DIRECT
Neurocomputing 69 (2006) 1125–1129
NEUROCOMPUTING
www.elsevier.com/locate/neucom

Effects of correlated input and electrical coupling on synchrony in fast-spiking cell networks

Abraham R. Schneider[a], Timothy J. Lewis[b,*], John Rinzel[a,c]

[a]Center for Neural Science, New York University, NY 10003, USA
[b]Department of Mathematics, University of California Davis, CA 95616, USA
[c]Courant Institute for Mathematical Sciences, New York University, NY 10003, USA

Available online 9 February 2006

Abstract

Fast-spiking (FS) cells in layer IV of the somatosensory cortex receive direct thalamocortical (TC) input and provide feed-forward inhibition onto layer IV excitatory cells. The level of synchronous firing of FS cells will affect the shape of this feed-forward output. Two factors that contribute to the synchrony are correlated TC input and electrical coupling between FS cells. Using a cell-pair model, we show that these two factors act synergistically to increase synchrony, and we examine the underlying mechanism.

Keywords: Inhibition; Synchrony; Electrical coupling; Correlated input; Fast-spiking cortical interneurons

1. Introduction

Sensory information provided by the whiskers of mice, rats, and rabbits is carried from barreloids in the ventroposterior medial thalamus (VPM) to barrels found in the primary somatosensory cortex (S1) [10]. Thalamocortical (TC) cells from the VPM form primary synapses with two types of cells in layer IV of the cortex: regular-spiking (RS) excitatory cells and fast-spiking (FS) inhibitory interneurons [3]. Because FS cells receive monosynaptic input from the TC cells and synapse directly on RS cells, they are thought to be responsible for fast feed-forward inhibition to the RS cells [6,14]. Therefore, the network of FS cells is believed to play an important role in information processing in the cortex [13]. To understand how information is transformed in this layer, it is essential to understand the dynamics in the FS cell network.

In vivo, FS cells in a single barrel often fire in sharp synchrony [17]. This suggests that an important attribute of the FS cells within a single barrel is that they act in concert. Indeed, the level of synchrony in the FS cell population will determine the temporal structure of the feed-forward inhibition and thus shape the activity of the RS cells. Several different network features could contribute to the observed correlation between FS cells. In the present study,

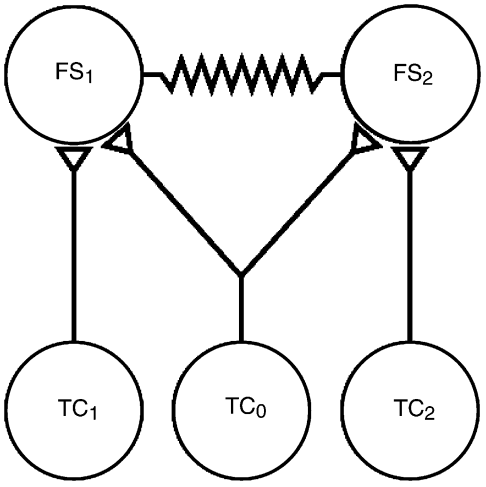

Fig. 1. Schematic diagram of the two cell model. Each FS cell receives input from an independent source (TC_1 or TC_2) and a common source (TC_0). The TC inputs are modeled as many homogenous Poisson processes with a total firing rate ranging from 0–3.3 kHz. Intrinsic dynamics of the FS cells are described by a spike-response model. The total input into each FS cell is kept constant, such that $TC_0 + TC_{1,2} = 3.3$ kHz.

*Corresponding author.
E-mail addresses: abes@cns.nyu.edu (A.R. Schneider), tjlewis@ucdavis.edu (T.J. Lewis).

0925-2312/$ - see front matter © 2006 Elsevier B.V. All rights reserved.
doi:10.1016/j.neucom.2005.12.058

we consider the effects of two factors that can contribute to synchronous firing: convergent input from diverging TC synapses [16–18] and the electrical coupling between FS cells [1,3,6]. Other possible factors that affect synchrony include feedback from RS cells [3] and inhibitory connections between FS cells [6,11,20]. However, we do not consider these factors here.

In previous work using a 400 FS cell network [15], we have shown that shared TC input or electrical coupling alone produces a small amount of correlated firing. However, if both factors are present, they produce a substantially larger correlation than would be predicted by simply adding the correlations obtained when electrical coupling and shared TC input are considered separately. In

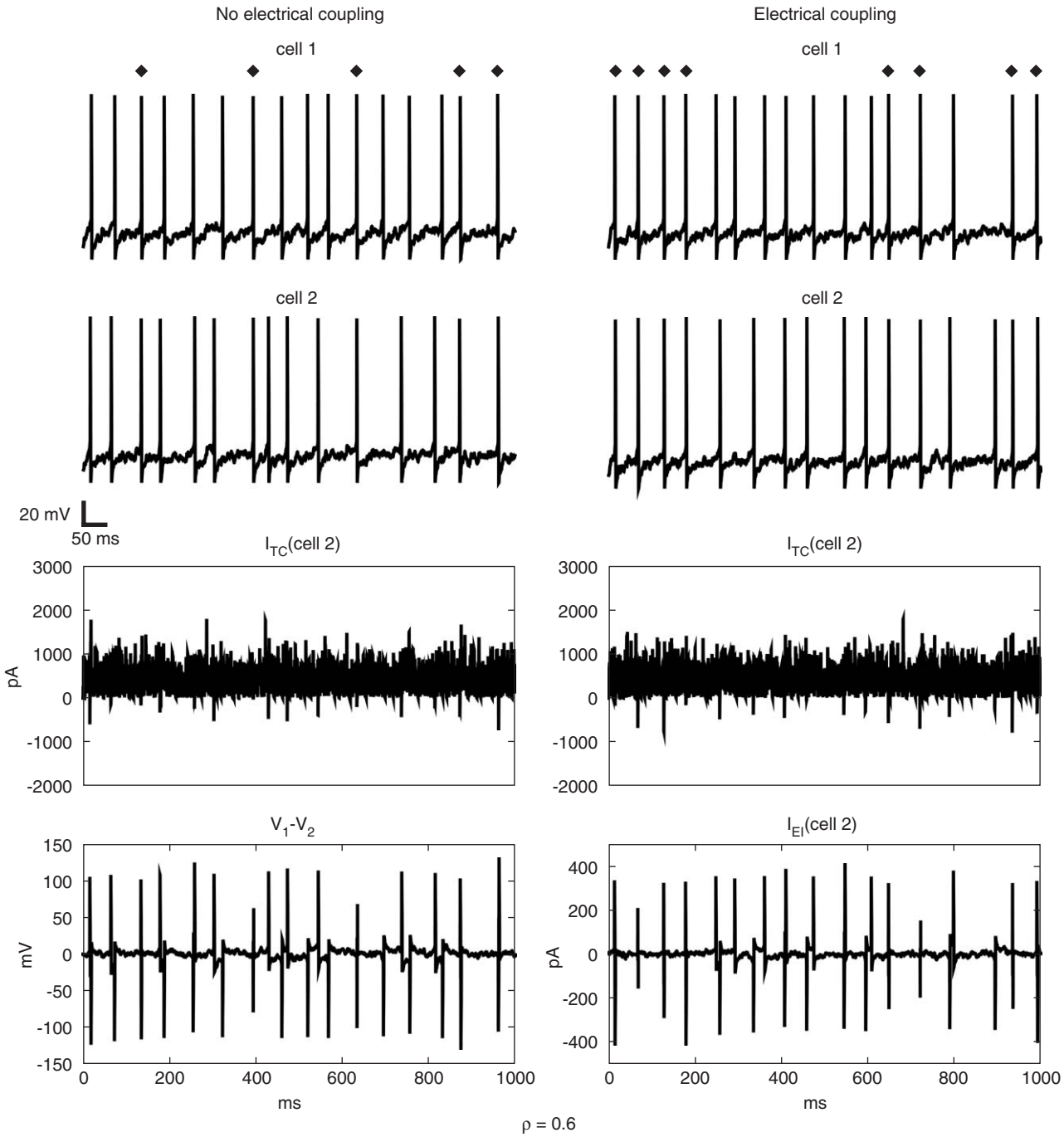

Fig. 2. Synaptic input into FS cells. First two rows show transmembrane potentials of the FS cells when TC input correlation $\rho = 0.6$ with electrical coupling ($g_{El} = 3$ nS) and without electrical coupling ($g_{El} = 0.0$ nS). Diamonds mark synchronous spikes between the two cells. The third row shows the TC input current (I_{TC}) to FS cell 2. On average, I_{TC} appears to be the same for both conditions. The last row shows $V_1 - V_2$ for the condition without electrical coupling, and I_{El} for the case with electrical coupling. Note that I_{TC} is much larger than I_{El}, and the large values for I_{El} are transitory.

this paper, we demonstrate the existence of this synergistic effect in a cell-pair model and use the model to identify the mechanisms underlying the effect.

2. Model description

Fig. 1 shows a schematic of the cell-pair model network. The intrinsic firing properties of the FS cells are described by a spike-response model for the FS cell [8], which is a direct reduction of a single-compartment conductance-based model for neocortical FS cells [4]. Parameters were picked to match experimental data as closely as possible. FS cells had a membrane resting potential of -74 mV [5], a threshold of $V_{TH} = -50$ mV [6], a resting membrane conductance of $g_m = 30$ nS, and a membrane time constant of 4 ms [3].

The electrical coupling current flowing from cell i to cell j is described by: $I_{El}(i,j) = g_{El}(V_i - V_j)$, where V_j is the membrane potential of cell j ($j = 1,2$). The coupling conductance g_{El} is defined as g_m [CC/(1−CC)], where the coupling coefficient (CC) is set to 0.095 [1]. Each FS cell has an independent TC input and a common TC input. The parameter ρ is the ratio of the common TC input to the total TC input into an FS cell and is used as a measure of the correlation of the TC input. The total TC input is kept constant so that the FS cells fire at a frequency of approximately 15 Hz [19]. Each TC input represents the firing of many TC cells and is modeled by describing the spontaneous firing times as independent homogeneous Poisson processes with a rate ranging between 0 and 3.3 kHz. A delta-function at each spike time is convolved with an alpha-function to give the synaptic input conductance to match 1 mV EPSPs in [3] ($\tau = 0.2$ s and $g_{TC} = 3.14$ nS).

Synchrony is defined as both cells firing an action potential within ± 1ms ($\Delta = 1$ ms) of each other. The level of synchrony is calculated by: $[(N_{coinc} - \langle N_{coinc} \rangle)/([1/2](N_1 + N_2))][1/M]$ [8], where N_1 is the number of spikes in the reference spike train, and N_2 is the number of spikes in the target spike train. N_{coinc} is the number of coincident spikes in two spike trains with a precision of Δ. $\langle N_{coinc} \rangle = 2\nu\Delta N_1$ is the mean number of spikes predicted by a homogenous Poisson process that has the same firing rate as cell 2. $M = 1 - 2\nu\Delta$ normalizes the correlation to a maximum of 1, where ν equals the firing rate of cell 2.

3. Results

The current due to TC input (I_{TC}) is much larger than that due to electrical coupling (I_{El}) (Fig. 2, lower traces). Although I_{El} can transiently reach values of up to 400 pA, this is still small in comparison to the driving I_{TC}. However, as shown in Fig. 2 (upper traces), the addition of electrical coupling can substantially increase the pairwise synchrony.

The top and bottom curves in Fig. 3 show the synchrony between the FS cells as a function of TC input correlation

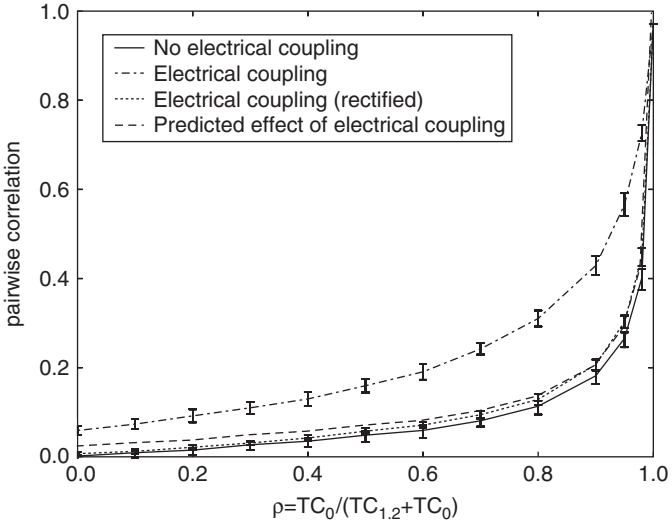

Fig. 3. Pairwise correlation between cells. Pairwise correlation as a function of TC input correlation (ρ). Bottom curve is without electrical coupling, top curve is with electrical coupling. Dashed line is predicted curve if electrical coupling and shared input added linearly. Dotted line is with rectifying electrical synapses that turn off above -58 mV. Errorbars show the standard deviation around the mean correlation across trials.

(ρ) for the conditions of electrical coupling and no electrical coupling, respectively. In both cases, output correlation increases with ρ. With weak electrical coupling alone, there is only a small amount of synchrony (0.06) as indicated by the correlation value at $\rho = 0$ in Fig. 3. If the effects of electrical coupling and TC input correlation were to sum linearly, the bottom curve would only be shifted up by the constant amount 0.06 (Fig. 3, dashed curve). However, the correlation when both shared TC input and electrical coupling are present is considerably above this line, indicating that these factors interact in a cooperative manner.

In order to understand the mechanism underlying this synergy between shared input and electrical coupling, we examine the spike-triggered averages (STA), triggered at $V_{TH} = -50$ mV, for both the input TC current and the difference in the cell's voltages ($V_{1-2} = V_1 - V_2$). Note that V_{1-2} is proportional to I_{El}. The STA of I_{TC} is invariant to changes in ρ, indicating that I_{TC} is not playing a role in the observed synergy (Fig. 4, column 1). For the STA of V_{1-2}, a negative trend is seen near $t = 0$ when electrical coupling is not present (Fig. 4, column 2, dashed line). This negative trend decreases with ρ. For low values of ρ, the cell's voltages will be relatively uncorrelated, and thus when cell 2 is near V_{TH}, it is unlikely that cell 1 is also close to V_{TH}. This causes V_{1-2} to be negative. As ρ increases, the two cell's voltages are more correlated. Thus, when V_2 is near V_{TH}, it is more likely that V_1 is near V_{TH}, causing V_{1-2} to be less negative. When electrical coupling is added, a negative trend near $t = 0$ is also observed for lower values of ρ. However, V_{1-2} flattens out faster, and a positive trend is seen for values of ρ above 0.6. If cell 1 fires an action potential when cell 2 is near threshold, then small

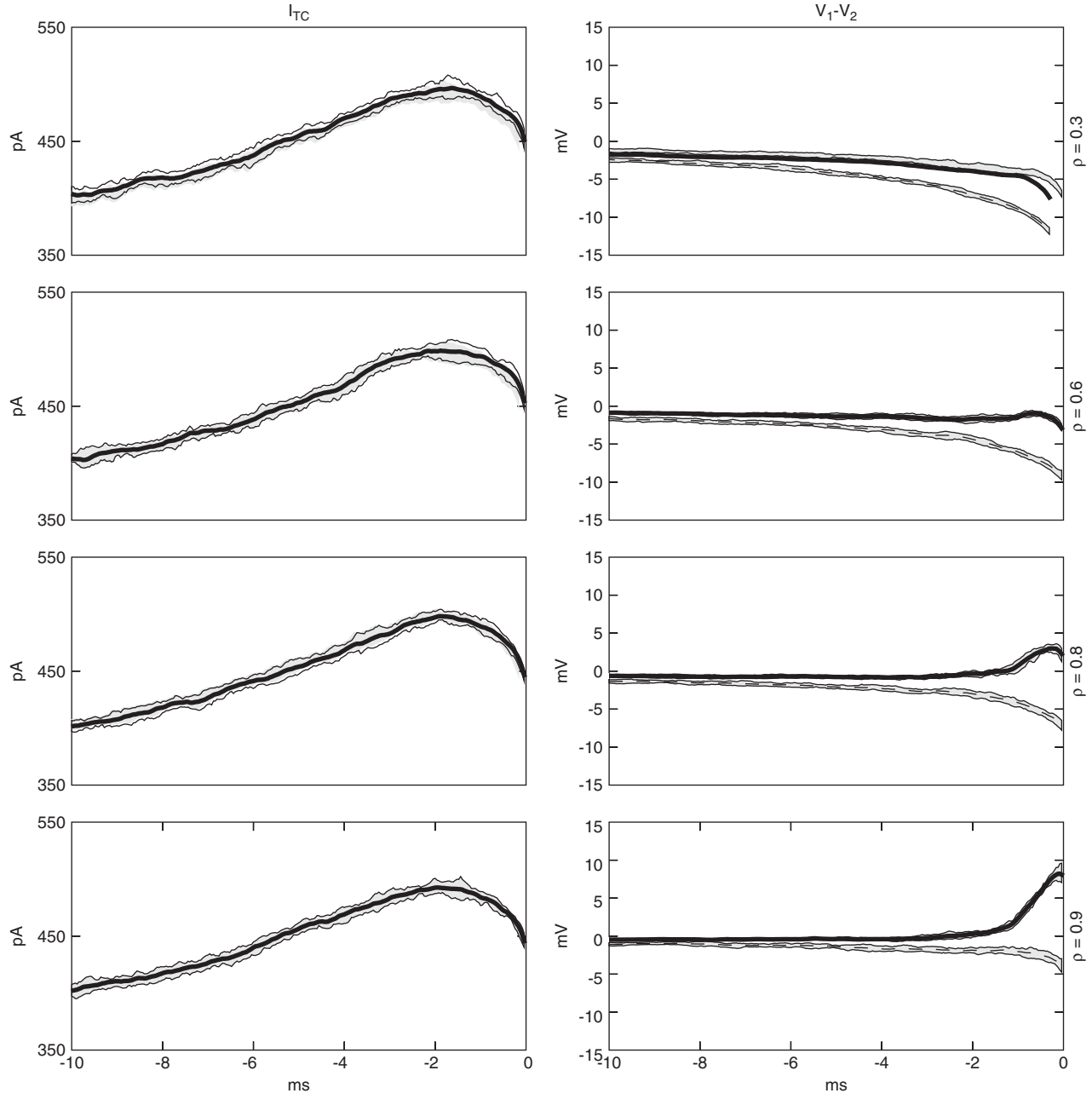

Fig. 4. Spike-triggered averages. Column 1 shows the spike-triggered average (STA) of the input TC current going into cell 2, when cell 2 fires an action potential (0 ms). Column 2 shows the STA of the differences in voltage between the two cells for the case with electrical coupling (solid thick line) and no electrical coupling (dashed line). Shaded area shows the standard deviation around the mean correlation across trials.

contributions from I_{El} can push cell 2 over threshold. If this event occurs at a high enough frequency, then a positive trend near $t = 0$ will be observed in the STA. If for low values of ρ, an STA is constructed from only synchronous events, a positive trend is also observed (data not shown).

When comparing the STAs of V_{1-2} with and without electrical coupling for a fixed ρ, a confounding factor is that the output correlation is different. It is possible that the difference in the STAs is solely due to this difference in correlation and the shape of the action potential. However, if we compare the STAs for the case with electrical coupling at $\rho = 0.6$ to the case without electrical coupling at $\rho = 0.9$, where both have the same output correlation ($\sim$0.2), then a difference in STAs for V_{1-2} can still be seen. This suggests that the positive trend is indeed due to contributions from I_{El}.

To examine the ability of electrical coupling to synchronize activity at subthreshold potentials, the electrical synapse was turned off when either V_1 or V_2 was above -58 mV. This eliminates any effect that action potentials have on synchronizing the cells [19]. The rectifying electrical synapse produces pairwise correlations (Fig. 3, dotted line) well below the linear summation prediction (Fig. 3, dashed line). Additionally, voltage-triggered

averages of V_{1-2} were constructed triggered at $V_2 = -60$ and -70 mV. These traces were nearly flat (data not shown), indicating that electrical coupling has very little effect on the cell's voltage at subthreshold levels.

4. Conclusions

We have found that the weak electrical coupling between FS cells can interact synergistically with shared TC input to substantially increase synchronous firing of the FS cells. This synergy is predominantly dependent on the effects of action potentials in FS cells. I_{El} is maximal when one cell fires an action potential, and a cell is most sensitive to perturbations when its membrane potential is close to threshold. Therefore, a cell that is near threshold can readily fire in response to I_{El} that is flowing from a cell undergoing an action potential. Correlation in the TC input can produce a loose synchrony that can bring cells close to threshold at similar times. This allows the electrical coupling to further synchronize the cells as described above, thus leading to the synergistic synchronizing effect of shared TC input and electrical coupling. Because electrical synapses are weak, I_{El} is small compared to the large I_{TC} fluctuations, and therefore subthreshold interactions through the electrical synapses have only a very small effect on synchronizing FS cell firing.

In this modeling study, we did not include recurrent inhibition between FS cells and feedback from the RS cells. Additionally, we have examined the model under spontaneous conditions only. To further understand the FS network's effect on incoming sensory information, it will be necessary to study the response to stimulus-evoked input in a more complete model of layer IV circuitry. However, we believe that the synergistic mechanism we describe here will carry over to more detailed models.

Acknowledgments

The work of John Rinzel was supported in part by NIH/NIMH Grant MH62595. Tim Lewis is supported by a grant from the National Science Foundation (NSF) Grant (DMS-0518022).

References

[1] Y. Amitai, J.R. Gibson, M. Beierlein, S.L. Patrick, A.M. Ho, B.W. Connors, D. Golomb, The spatial dimensions of electrically coupled networks of interneurons in the neocortex, J. Neurosci. 22 (2002) 4142–4152.

[3] M. Beierlein, J.R. Gibson, B.W. Connors, Two dynamically distinct inhibitory networks in layer 4 of the neocortex, J. Neurophysiol. 90 (2003) 2987–3000.

[4] A. Erisir, D. Lau, B. Rudy, C.S. Leonard, Function of specific K^+ channels in sustained high-frequency firing of fast-spiking neocortical interneurons, J. Neurophysiol. 82 (1999) 2476–2489.

[5] M. Galarreta, S. Hestrin. Electrical, chemical synapses among parvalbumin fast-spiking GABAergic interneurons in adult mouse neocortex, PNAS 99 (2002) 12438–12443.

[6] J.R. Gibson, M. Beierlein, B.W. Connors, Two networks of electrically coupled inhibitory neurons in neocortex, Nature 402 (1999) 75–79.

[8] R. Jolivet, T.J. Lewis, W. Gerstner, Generalized integrate-and-fire models of neuronal activity approximate spike trains of a detailed model to a high degree of accuracy, J. Neurophysiol. 92 (2004) 959–976.

[10] P.W. Land, S.A. Buffer, J.D. Yaskosky, Barreloids in adult rat thalamus: three-dimensional architecture and relationship to somatosensory cortical barrels, J. Comp. Neurol. 355 (1995) 573–588.

[11] T.J. Lewis, J. Rinzel, Dynamics of spiking neurons connected by both inhibitory and electrical coupling, J. Comput. Neurosci. 14 (2003) 283–309.

[13] D.J. Pinto, J.C. Brumberg, D.J. Simons, Circuit dynamics and coding strategies in rodent somatosensory cortex, J. Neurophys. 83 (2000) 1158–1166.

[14] J.T. Porter, C.K. Johnson, A. Agmon, Diverse types of interneurons generate thalamus-evoked feedforward inhibition in the mouse barrel cortex, J. Neurosci. 21 (8) (2001) 2699–2710.

[15] A.R. Schneider, T.J. Lewis, H.A. Swadlow, J. Rinzel, The influence of electrical coupling on synchrony in fast-spiking interneurons in layer 4 neocortex, Society for Neuroscience, 2004.

[16] H.A. Swadlow, Influence of vpm afferents on putative inhibitory interneurons in s1 of the awake rabbit: evidence from cross-correlation, microstimulation, and latencies to peripheral sensory stimulation, J. Neurophysiol. 73 (1995) 1584–1599.

[17] H.A. Swadlow, I.N. Beloozerova, M.G. Sirota, Sharp, local synchrony among putative feed-forward inhibitory interneurons of rabbit somatosensory cortex, J. Neurophysiol. 79 (1998) 567–582.

[18] H.A. Swadlow, A.G. Gusev, Receptive-field construction in cortical inhibitory interneurons, Nat. Neurosci. 5 (2002) 403–404.

[19] R.D. Traub, N. Kopell, A. Bibbig, E.H. Buhl, F.E.N. LeBeau, M.A. Whittington, Gap junctions between interneuron dendrites can enhance synchrony of gamma oscillations in distributed networks, J. Neurosci. 21 (2001) 9478–9486.

[20] X.J. Wang, G. Buzsaki, Gamma oscillation by synaptic inhibition in a hippocampal interneuronal network model, J. Neurosci. 16 (1996) 6402–6413.

John Rinzel is a Professor in the Center for Neural Science and Courant Institute for Mathematical Sciences at New York University. He received his Ph.D. from NYU in 1973 and was a scientist and Lab Chief of the Mathematical Research Branch (NIDDK) at the National Institutes of Health until 1997.

Abraham Schneider is a graduate student in the Center for Neural Science at New York University. He received a BS/BA in Neuroscience and Computer Science from Brandeis University in 2001.

Tim Lewis is an Assistant Professor in the Department of Mathematics at the University of California, Davis. He received a Masters degree in Physiology at McGill University and a Ph.D. in Mathematics at the University of Utah. He was a postdoctoral fellow at New York University with John Rinzel until 2004.